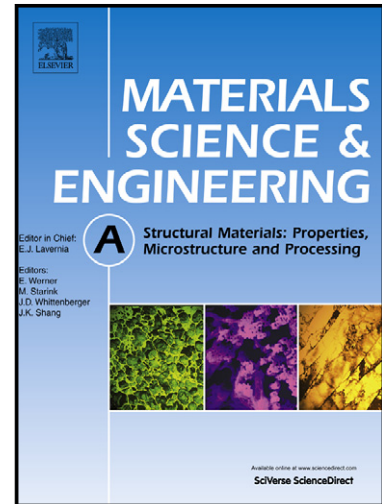


Author's Accepted Manuscript

Effect of two-pass friction stir processing on the microstructure and mechanical properties of as-cast binary Al-12Si alloy

S.M. Aktarer, D.M. Sekban, O. Saray, T. Kucukomeroglu, Z.Y. Ma, G. Purcek



www.elsevier.com/locate/msea

PII: S0921-5093(15)00371-8
DOI: <http://dx.doi.org/10.1016/j.msea.2015.03.111>
Reference: MSA32208

To appear in: *Materials Science & Engineering A*

Received date: 11 February 2015
Revised date: 27 March 2015
Accepted date: 29 March 2015

Cite this article as: S.M. Aktarer, D.M. Sekban, O. Saray, T. Kucukomeroglu, Z.Y. Ma, G. Purcek, Effect of two-pass friction stir processing on the microstructure and mechanical properties of as-cast binary Al-12Si alloy, *Materials Science & Engineering A*, <http://dx.doi.org/10.1016/j.msea.2015.03.111>

This is a PDF file of an unedited manuscript that has been accepted for publication. As a service to our customers we are providing this early version of the manuscript. The manuscript will undergo copyediting, typesetting, and review of the resulting galley proof before it is published in its final citable form. Please note that during the production process errors may be discovered which could affect the content, and all legal disclaimers that apply to the journal pertain.

Effect of two-pass friction stir processing on the microstructure and mechanical properties of as-cast binary Al-12Si alloy

S.M. Aktarer^a, D.M. Sekban^b, O. Saray^c, T. Kucukomeroglu^d, Z.Y. Ma^c, G. Purcek^{d,*}

^aDepartment of Automotive Technology , RecepTayyip Erdogan University, Rize, Turkey

^bDepartment of Naval Architecture and Marine Engineering, Karadeniz Technical University, Trabzon, Turkey

^cDepartment of Mechanical Engineering, Bursa Technical University, Bursa, Turkey

^dDepartment of Mechanical Engineering, Karadeniz Technical University, Trabzon, Turkey

^eShenyang National Laboratory for Materials Science, Institute of Metal Research, Chinese Academy of Sciences, Shenyang, China

Abstract

The effect of two-pass friction stir processing (FSP) on the microstructural evolution, mechanical properties and impact toughness of as-cast Al-12Si alloy was investigated systematically. Severe plastic deformation imposed by FSP resulted in a considerable fragmentation of the needle-shaped eutectic silicon particles into the smaller ones. The length of eutectic Si particles decreased from 27 ± 23 μm to about 2.6 ± 2.4 μm . The average aspect ratio of 6.1 ± 5.1 for eutectic Si particles in the as-cast state decreased to about 2.6 ± 1.0 after FSP with a corresponding increase in their roundness. The hardness, strength, ductility and impact toughness of the alloy increased simultaneously after two-pass FSP. The increase in the yield and tensile strength values after FSP was about 20% and 29%, respectively. The FSPed alloy exhibited 25% elongation to failure and 15% uniform elongation which were almost seven times and five times higher, respectively, than those of the as-cast alloy. The hardness of the alloy increased from 58 Hv0.5 for the as-cast state to about 67 Hv0.5 after FSP. The absorbed energy during impact test increased to about 8.3 J/cm² after FSP, which is about seven times higher than that of the as-cast alloy. Improvements in all mechanical properties were mainly attributed to the radical changes of the shape, size and distribution of the eutectic silicon particles along with the breakage and refined of the large α -Al grains during two-pass FSP.

Keywords: Friction stir processing, Al-12Si alloy, microstructure, hardness, tensile properties, impact toughness.

*Corresponding author. Tel.: +90-4623772941; Fax: +90-4623253336

E-mail address: purcek@ktu.edu.tr (G. Purcek)

1. Introduction

Al-Si alloys have good engineering properties, such as superior wear resistance, low thermal expansion coefficient, high corrosion resistance, high strength-to-weight ratio and excellent castability [1-5]. Thus, they are widely used especially in automotive, aerospace and military applications [2]. However, their insufficient strength, very poor ductility and low fracture toughness in the as-cast condition impede their broader applications [2, 6, 7]. Some traditional approaches have been undertaken in order to minimize their aforementioned problems. For this purpose, alloying with different elements, heat treatments, controlling casting parameters, grain refinement and modification during solidification and/or post-solidification have been applied so far [5-8]. Although some improvements in their properties have been achieved, it is still needed to improve their strength, ductility and impact toughness [1, 2]. Therefore, some new applicable approaches should be put forward to enhance their potential applications. Grain refinement and/or grain modification by plastic deformation are thought to be a strong alternative for this purpose. But classical plastic deformation processes, such as extrusion, forging and rolling have serious limitations for achieving substantial grain refinement which would lead to improvement in mechanical properties of Al-Si alloys [1, 7, 9].

Recently, new grain refinement and microstructural modification techniques based on severe plastic deformation (SPD) have been proposed in order to overcome some of the challenges of conventional metal forming processes [10, 11]. Among SPD methods, equal-channel angular pressing/extrusion (ECAP/E), high pressure torsion (HPT), accumulative roll-bonding (ARB) and friction stir processing (FSP) are well known ones [10-12]. The FSP is the best one among others as considering the processing of large-scale plate- or sheet-type materials.

FSP is a method of changing the properties of a material through severe, localized plastic deformation which is produced by forcibly inserting a non-consumable tool into the work piece, and revolving the tool in a stirring motion as it is pushed laterally through the work piece [13-15]. The precursor of this technique, friction stir welding (FSW), is utilized to join multiple pieces of similar

and dissimilar materials. This process mixes a material without changing its phase structure and creates a microstructure with fine, equiaxed and uniformly distributed grains. The processed zone is constituted generally by recrystallized fine grains, fragmented primary particles and uniformly distributed second phase particles. Many research and also review papers on this process have been published up to now, and thus detailed information on its principles can be obtained in Refs. [13-16].

FSP method has been applied to Al-Si alloys with or without secondary alloying elements in the hypoeutectic [17-21], near eutectic [22-25] and hypereutectic compositions [26, 27]. The most of them have focused on the microstructural evolution and mechanical characteristics of plastic deformation during FSP. Generally, it was reported that FSP improves mechanical properties of as-cast Al-based alloys and achieves significant microstructural refinement [2, 17, 22, 23, 24]. A detailed study on the microstructural development of Al-7SiMg (A356) alloy during FSP was carried out by Ma *et al.* [17]. They found that as-cast microstructure is homogenized and refined by FSP, and this process generated fine Si particles distributed in a fine-grained α -Al matrix. In addition, the fatigue and crack growth behaviors [18, 28, 29, 30], microstructural modification [2, 17, 27, 31], mechanical properties [25, 32, 33, 34], superplasticity [35] and wear behavior [36] of A356 Al-Si standard alloy have been investigated after FSP.

Mahmoud [26] reported that the size and aspect ratio of Si particles of hypereutectic as-cast Al-Si alloys decreased from 59 ± 24 μm to about 4.39 ± 1.9 μm and from 3.56 ± 1.9 μm to about 1.18 ± 0.4 μm , respectively. Rao *et al.* [27] observed more uniform microhardness in the stir zone (SZ) of FSPed hypereutectic as-cast Al-30Si alloy than that of the as-cast one. Several researchers have also carried out some studies on near-eutectic and eutectic Al-Si alloys. Mahmoud *et al.* [24] investigated the effect of FSP on the mechanical and tribological characteristics of A413 as-cast Al alloys. They found that the wear resistance, hardness and strength of the FSPed region decreased by increasing the tool rotation speed while the ductility increased about 1.6–2.7 times. Tsai and Kao [20] reported that the tensile strength and elongation to failure of FSPed AC8A alloy increased from

159 to 322 MPa and from 0.9% to 15.4%, respectively, under the parameters of 1400 rpm and 45 mm/min. They also found that high tool rotation rate enhanced the dissolution of β' and Q' particles while low tool rotation rate in FSP brought about a precipitate coarsening [20]. Tutunchilar *et al.* [23] used the FSP in order to change the surface of eutectic LM13 Al–Si alloy to hypereutectic alloy by putting 10% volume fraction of Si particles. They reported that the hardness increased with the first pass of FSP of the as-cast alloy, but the hardness reduced during subsequent passes, which was related to the dissolution of precipitates such as Mg_2Si . Rayesa *et al.* [21] showed that an increase in the number of passes during processing of commercial 6082 Al alloy reduced the tensile strength of the SZ while increasing the traverse speed increased the mean hardness and tensile strength of the SZ. Wais *et al.* [22] reported that the strength and elongation of FSPed sand casted eutectic Al-12Si alloy increased from 123 MPa to 160 MPa and from 5.8% to 14.5%, respectively.

In view of above, there are many reports on FSP of Al-Si alloys containing different additional alloying elements. However, very limited studies have been undertaken on the as-cast binary Al-Si alloys. Also, the effect of FSP on the microstructural evolution with quantitative measurements and mechanical properties, including the combination of strength, ductility and also impact toughness of the as-cast Al–Si alloys has not been investigated systematically [22]. Furthermore, more studies are needed for getting further improvement in mechanical properties (especially in the impact toughness and ductility) of Al-Si alloys by applying FSP with optimum parameters. Therefore, the main purpose of this study is to modify the surface structure of as-cast Al-12Si alloy by FSP, and investigate its effect on the microstructural and mechanical properties in detail. Also, the changes in fractures mechanism before and after FSP were examined.

2. Experimental procedures

2.1. Materials and processing

In this study, a eutectic Al-12%Si alloy was produced by ingot casting metallurgy with a chemical composition of 12.2%Si, 0.6%Fe, 0.1%Cu, 0.4%Mn, 0.1%Mg, 0.1%Zn, 0.1%Ni, 0.15%Ti, 0.1%Pb, 0.05%Sn and balance Al. The ingots were re-melted in a graphite crucible for producing uniform as-cast microstructure and poured from 650°C into a mild steel permanent mold stayed at room temperature. Plates with the dimensions of 200 mm x 40 mm x 5 mm were machined from the ingots for FSP. FSP was performed using a tool steel with a shoulder diameter of 16 mm, a threaded pin with the diameter of 5 mm and length of 2.5 mm. During processing, the tool rotation and traverse speed were fixed at 1250 rpm and 65 mm.min⁻¹, respectively. The tool was tilted 3°, and downforce of the tool was kept constant at 3 kN. Two-pass FSP was applied to the alloy plate in order to introduce homogeneous deformation into the processed zone during FSP and achieve finer and homogeneously distributed Si particles. First pass was carried out in the process direction as shown in Fig. 1. After first pass, the FSP tool was unloaded and the second pass was performed through the pre-processed region by placing the tool at the starting point of the first pass again.

Samples for metallographic investigation were sectioned perpendicular to the process direction of plate and then prepared using standard polishing techniques before etching in a 10% NaOH solution (Fig. 1). Microstructural characteristic of the alloy before and after FSP were investigated using optical microscopy. Quantitative measurements of the size of eutectic silicon particles and their aspect ratio were conducted using image analysis software.

Tensile tests were performed using dog-bone shaped tension samples with the dimensions of 2 mm x 5 mm x 26 mm machined from the processed plates where their tensile axis were oriented parallel to the process direction (Fig. 1). The tests were performed using an Instron-3382 electro-mechanical load frame at a strain rate of $5.4 \times 10^{-4} \text{ s}^{-1}$. Strain was measured using a video type extensometer. For each case, three experiments were conducted on companion specimens to check

the repeatability of the results. Fracture surfaces and sub-surfaces of the tension samples were examined using a JEOL-6400 scanning electron microscope (SEM) before and after FSP in order to verify the possible changes in their deformation mechanism. Hardness measurements were performed using a Vickers micro-hardness tester operated at $H_V0.5$. The measurements were carried out on both longitudinal and transverse sections of processed plate (Fig. 1).

The impact toughness of the alloy was evaluated by measuring the total absorbed energy using Charpy impact test before and after FSP. The samples with the dimensions of 3 mm x 4 mm x 27 mm (DIN50115) were cut from the FSPed plate perpendicular to the process direction (Fig. 1). Surfaces of the fractured samples were also investigated using SEM.

3. Results and discussion

3.1. Microstructural evolution

Optical micrographs of as-cast Al-12Si alloy before FSP are shown in Fig. 2(a)-(b). The microstructure of as-cast alloy consists of eutectic Si particles (dark color), α -Al phase (white color), and few coarse primary silicon particles (dark color). Eutectic Si particles exhibit a fibrous morphology in the form of acicular or needle-shaped plates dispersed throughout the α -Al matrix. Limited large primary Si particles are also observed in the microstructure due to the non-equilibrium cooling and slightly variations in the eutectic composition. This is a typical structure of as-cast eutectic Al-Si alloy [1, 17].

The effect of FSP on the microstructure of as-cast Al-12Si alloy is shown in Fig. 3(a)-(g). It is apparent that the effect of FSP on the shape, size and size distribution of eutectic Si particles dispersed in the matrix is more pronounced compared to other constituents. Two distinct zones were formed in the processed region: The nugget zone (NZ) and the thermo-mechanically affected zone (TMAZ) formed due to the severe plastic deformation, friction-induced high temperature causing recrystallization and complicated material flow during FSP. The needle-shaped eutectic Si particles

are severely broken in the NZ by stirring movement of the tool during FSP because of the brittle nature of these particles. After two-pass FSP, the Si particles became nearly equiaxed in shape and uniformly distributed in size inside the NZ [3, 17]. The change in coarse primary Si particles is inconsiderable during FSP in that zone.

It is worthy to note that the TMAZ can be divided into two sub-regions depending on the forming places. A region is formed primary by the effect of shoulder on the top most layer just below the shoulder (Fig. 3(b)), which can be named as “shoulder-affected (SE) TMAZ”. The region formed along the NZ inside the processed region can be called as “pin-affected (PE) TMAZ”. It is clearly seen that The SE-TMAZ forms along the shoulder diameter (Fig. 3(a)). Therefore, an intense deformation under the compressive stress of shoulder is much more effective in that region during FSP. This region is influenced by relatively high temperature generated by intense frictional effect occurring inside the material and also the interaction of the surfaces of the sample and shoulder. The stirring effect of the pin is not very effective in that zone. These effects bring about a less-fractured and coarsened-Si particles and α -Al matrix as shown in Fig. 3(b). Actually, this layer was neglected almost in all previous reports. But, it seems to be inevitable during FSP of such kind of soft materials. In the PE-TMAZ, the stirring effect of the pin is much more pronounced compared to the SE-TMAZ. The transition region between the NZ and the PE-TMAZ is shown in the Fig. 3(e)-(g). From these figures, a distinct transition is obvious between the NZ and the PE-TMAZ. Silicon particles in that zone are coarser with relatively high aspect ratio since it is subject to less severe plastic deformation than the NZ as in the case of the SE-TMAZ. Also, eutectic Si particles in that region are aligned parallel to the process direction (Fig. 3(f)-(g)). Although the TMAZ undergoes plastic deformation, recrystallization did not fully occur in that zone due to insufficient deformation strain as reported by Mishra et al. [15]. The structure in Fig.3 (e)-(g) shows a partial recrystallization where some fine Si particles started forming within the elongated Si particles. Such structural formation has also been reported in many other Al alloys [2, 21, 23].

Size distribution of the length of eutectic Si particles before and after FSP are shown in Fig. 4. Almost all Si particles' length is over 5 μm , and a majority of them lies in the size range of 10-50 μm in the as-cast alloy (Fig. 4(a)). A considerable amount of eutectic particles (over 16%) have the sizes above 50 μm . The average length of eutectic silicon particles in the as-cast alloy is 27 ± 23 μm , which means that the eutectic Si particles of as-cast alloy are in the form of coarse and needle-shaped. It is apparent that there is a significant reduction in the length of silicon particles by the effect of FSP; that is, it decreases from 27 ± 23 μm to about 2.6 ± 2.4 μm after two-pass FSP. Over the length of 34% eutectic Si particles is equal or smaller than 1 μm , and the fraction of Si particles with the size less than 8 μm is as high as 95% after two-pass FSP.

The change in the morphology of eutectic Si particles inside the NZ by FSP was also characterized by the aspect ratio (the length-to-width ratio) as shown in Fig. 5. It is seen that two-pass FSP has a significant influence on the aspect ratio of the eutectic Si particles in that zone. The aspect ratio decreases due to the breaking of eutectic Si particles in the direction of length during FSP [2, 18, 26, 27, 32]. The average aspect ratio of 6.1 ± 5.2 for the eutectic Si particles in the as-cast condition decreases to about 2.6 ± 1.0 after two-pass FSP. It was not measured quantitatively, but this change in aspect ratio is accompanied by a corresponding increase in the roundness of the particles as observed in Fig. 3(b)-(d). This indicates that the eutectic Si particles become more spherical by the effect of FSP as expected.

3.2. Mechanical Properties

3.2.1. Microhardness

Microhardness profiles of the FSPed sample through the vertical and longitudinal sections of the processed plate are shown in Figs. 6(a)-(d). The hardness profiles indicate the formation of distinct zones through the sections of FSPed sample as explained above (Fig. 6) [19, 21,37]. From Fig. 6, the highest hardness was measured in the NZ, this dropped suddenly in the SE-TMAZ and PE-TMAZ and finally reached to about the value of base material. The un-affected zone exhibited

hardness values in the range of 51-65 Hv0.5, which indicates highly scattered hardness distribution inside the as-cast structure. The average value is 58 Hv0.5 for the as-cast structure. This is a normal as considering the inhomogeneous distribution of coarse eutectic Si particles as well as casting segregation inside the as-cast microstructure [19, 34] (Fig. 2).

Two-pass FSP considerably increased the hardness of the alloy inside the NZ. The sample shows an increase in the hardness of about 15%, from 58Hv0.5 in the un-processed as-cast zone to about 67 Hv0.5 in the NZ. This is primarily due to the increase in dispersion hardening of refined and more uniformly distributed eutectic silicon particles in the α -Al matrix by the effect of FSP [24,34]. Also, the α -Al matrix phase was refined due to the dynamic recrystallization during FSP [13, 15], which provide additional improvement in hardness of this zone [19]. The NZ zone, on the other hand, has more uniform hardness distribution (ranges from 63 Hv0.5 to 67 Hv0.5) with fewer scatter compared to the as-cast state as reported before [24, 26, 27, 32, 34]. This can be attributed to the fine and more uniformly distributed eutectic Si particles in the NZ of FSPed sample. The TMAZ has lower hardness values compared to the NZ even below the value of un-processed region. Its reason is not fully understood, but this can be explained in terms of differences in microstructural alterations through the processed zone during FSP [19]. Since the TMAZ is characterized by a less deformed structure, less fractured Si particles as well as coarse α -Al matrix, which leads to less dispersion of silicon particles bringing about softening [19, 34]. Similar microstructure and mechanical properties were also reported by Karthikeyan *et. al.* [19] and Choi *et. al.* [34].

3.2.2. Tensile Properties

The engineering stress-strain curves of the Al-12Si alloy before and after FSP are shown in Fig. 7, and the values of strength and ductility obtained from these curves are given in Table 1. As-cast alloy exhibited a typical stress-strain curve for a brittle material with very poor uniform and total elongations. After FSP, this curve changed to a typical ductile material's curve with a large

strain hardening region. Therefore, the strength and ductility of the alloy increased simultaneously by the effect of FSP. The sample showed an increase in the ultimate tensile strength (σ_{UTS}) of about 29%, from 167 MPa for the as-cast state to about 215 MPa for the FSPed state. Similarly, the yield strength (σ_Y) increased about 20% after FSP, from 109 MPa to 131 MPa. In addition, while the σ_{UTS}/σ_Y ratio is 1.53 in the as-cast alloy, it increased to about 1.64 after FSP, which meant that the strain hardening region increased with FSP. The ductility of the alloy also increased substantially after FSP. The FSPed sample exhibited considerably higher elongation to fracture (ϵ_f) of about 25% in comparison with as-cast sample having only 3.4%, which means that the ductility of FSPed sample was almost 7.4 times higher than that of the as-cast sample. More importantly, uniform elongation (ϵ_u) increased considerably after FSP in contrast to other UFG materials. It increased from 2.7% in the as-cast state to about 15% after FSP.

The simultaneous increase in strength and ductility after FSP can be attributed to the radical changes in the microstructure of the alloy during FSP. It is well known that the mechanical properties of Al-Si alloys strongly depend on the shape, size and distribution of silicon particles, porosities and also the size of α -Al matrix phase [1, 2, 24, 26, 32]. Needle shaped silicon particles dispersed in the matrix act as an internal stress raiser, which raises the cracking tendency of the alloy. Therefore, the as-cast alloy exhibited low strength and very poor ductility. During FSP, the as-cast morphology is completely broken up especially in the NZ (Figs. 2 and 3). The extensive friction stir effect during processing results in significant changes in Si morphology by breaking them into smaller particles. Finally, disintegration/fragmentation and better distribution of eutectic silicon particles form in the matrix after FSP, which leads to extraordinary improvement in strength and ductility of the alloy. It is not clearly seen in the micrographs in Fig.2, but it is well known that the casting morphology generally includes compositional segregation and micro-porosities [2, 26]. This morphology was also mostly eliminated, and instead a relatively sound structure was formed especially inside the NZ during deformation- and temperature-induced structural alterations (Fig. 3). Furthermore, significant frictional heating and intense plastic deformation during FSP lead to a dynamic recrystallization in

the NZ which results in more refined and equiaxed Al-rich α -grains [13], which gives an additional improvement in both strength and ductility of the FSPed sample.

Considering previous studies in literature, few reports [2, 22, 33] have focussed on the effect of FSP on the tensile properties of binary as-cast Al-Si alloys. Only one of them aimed the tensile properties of as-cast Al-12 Si alloy [22]. The strength values obtained in that study would be comparable [22]. However, the ductility values (ϵ_f and ϵ_u values) obtained in the present study is higher than those obtained in that study[22]. It was found an elongation to failure of 14.5% after FSP, which is much lower than that obtained (around 25% elongation to failure) in the present study. The second paper including tensile behavior was on the FSP of as-cast binary Al-7Si alloy [33]. But, the results obtained in that study are not feasible to compare with those obtained in the current work due to the difference in chemical composition.

Fracture surfaces of the as-cast and FSPed tension samples are shown in Fig. 8. The surface of as-cast sample is rough and it shows facets which indicate the brittle fracture mode due to the large α -Al grains including needle-shaped eutectic silicon particles (Fig. 8(a)) [2, 23, 24]. After FSP, characteristic of fracture surface entirely changed from brittle to ductile mode (Fig. 8(b)). As clearly seen in Fig. 8, the fracture surface has micro-voids and fine dimples which indicate a typical ductile fracture. During FSP, the needle-like eutectic Si particles were broken up with grain refinement as explained before [2, 23, 24]. Also, the broken Si particles were uniformly distributed throughout the microstructure. All these changes in the microstructure resulted in a radical changes in the fracture mode of the alloy from brittle to ductile. The stress-strain curves also confirm this formation by leaving a large background after FSP (Fig. 7). It can be said that the presence of needle-like silicon particles promotes a tendency towards brittle fracture, and thus as-cast alloys sample shows relatively low tensile elongation. After FSP, fine Si particles fragmented with low aspect ratio inside the refined matrix phase bring about a ductile fracture with relatively high tensile elongation [18, 20, 22, 23, 24, 30, 32].

Cross-sectional views showing the crack growth paths of failed as-cast and FSPed tensile samples are shown in Fig. 9. The crack in the as-cast sample propagates almost along the eutectic silicon plates (Fig. 9(a)). Damage is initiated by cracking of eutectic Si needles at small plastic strain during tension of the as-cast sample [2, 13, 28, 37]. Small cracks and voids created between the Si particles coalesce to generate a crack that propagates along the Si particles during subsequent progress in tension due to their poor bonding compared to the intradendritic regions [28]. The FSPed sample exhibited a different crack growth path (Fig. 9(b)). As explained, the needle-shaped Si particles are broken into the smaller and uniformly distributed particles (Fig. 3) during FSP. Therefore, further fragmentation during subsequent tension tests becomes improbable as explained by Garcia-Infanta *et al.* [5]. In the present study, initiation of voids during tension is not related to the fracture of Si particles but matrix ductile fracture by the nucleation of voids in potential sites such as the Si particle-Al matrix interfaces [1, 2]. Thus, the crack path in the FSPed sample is not completely along the Si particles but it is mostly through the Al-rich α -phase [1, 28, 37].

3.2.3. Impact Toughness

The effect of FSP on the impact toughness of as-cast Al-12Si alloy was studied for the first time and the results are shown in Fig. 10. Morphological features of the fracture surfaces in the macro- and micro-scales are also shown in Fig. 11. The as-cast alloy has very low absorbed energy of about 1.2 J/cm^2 . The impact toughness of the alloy increased notably by FSP. The absorbed energy of FSPed alloy is about 8.3 J/cm^2 , which is almost seven times higher than that of the as-cast one. This increment rate is almost the same with that of the ϵ_f (7.4 times), which indicates that there is a good relationship between impact toughness and tensile ductility of FSPed Al-12Si alloy. This significant improvement in the impact toughness of alloy is related to the microstructural changes formed during FSP. Mainly, the shape, size and size distribution of the eutectic silicon morphology govern the impact of the Al-Si alloys [2, 26, 28]. As-cast alloy consisted of eutectic mixture of plate-

shaped Si particles and α -Al matrix phase (Fig. 3.). Unmodified acicular silicon particles behave internal stress risers in the microstructure and provide easy path for fracture, which is the primary reason for the low impact toughness of the alloy [1, 13]. The fracture surface of the as-cast sample also supports this conclusion (Fig.11(a) and (c)). The fracture surface of the as-cast impacted sample consists of needle-shaped eutectic silicon particles inside the large α -Al grains. Hence, the surface is rough and shows many facets (not dimples). Fracture surface of as-cast alloy shows that the crack path follows mainly along the eutectic Si particles as in the case of tensile test sample (Fig. 9(a)) in consequence with higher tendency to crack nucleation and propagation. During impact testing of the as-cast alloy, damage appears by forming the cracks in-between the eutectic Si particles and α -phases at small strains. As the strain continues, small cracks and voids generate a large crack that propagates mainly along the acicular Si particles, which offers less resistance to crack propagation than the α -Al phase that leads to brittle fracture mode. This is also seen in the fractured sample without considerable reduction of cross-sectional area due to brittle fracture (Fig. 11(a)).

After FSP, the crack propagation mode considerably changed (Fig. 11(b) and (d)). The as-cast microstructure of the alloy was completely eliminated in processed zone after processing, and the needle-shaped eutectic silicon particles changed into uniformly distributed finer particles (Fig.3.) that improves both strength and ductility of the matrix as explained before (Table 1). Furthermore, FSP results in grain refinement of matrix phase due to deformation and temperature-induced dynamic recrystallization. It is well known that such type of microstructure in Al-Si alloys can inhibit the crack initiation and growth which brings about improving in impact toughness [1, 13,15]. The crack path of the FSPed sample also validates this results (Fig. 11(b) and (d)). The crack path of FSPed sample is relatively smooth, and its propagation takes place through the α -Al phase and Si particles. Also, the primary Si particles are clearly seen on the crack paths located mainly in Al- α phase. After FSP, the fracture surface changed to a fine dimpled rupture mode and exhibited a ductile fracture mode including more homogeneous fine dimples (Fig. 11(d)).

4. Conclusions

As-cast Al-12Si eutectic alloy was subjected to two-pass friction-stir processing (FSP), and its effect on the microstructure, hardness, tensile behaviour and impact toughness of the alloy were investigated systematically. The main conclusions of this study can be summarized as follows:

1. FSP leads to the fragmentation of needle-shaped silicon plates into the smaller and more uniformly distributed particles inside nugget zone (NZ). The average length of eutectic Si particles decreases from $27\pm 23\ \mu\text{m}$ in the as-cast state to about $2.6\pm 2.4\ \mu\text{m}$ in the FSPed state due to the breaking of eutectic Si particles in the direction of length during FSP.
2. The microstructural modification by FSP increases simultaneously the strength, ductility, hardness and impact toughness of the as-cast Al-12Si alloy. The FSPed sample exhibits a tensile strength of about 215 MPa and a yield strength of about 131 MPa, which are about 29% and 20% higher than those of as-cast alloy, respectively. Elongation to failure of the alloy increases from 3.4% in the as-cast state to about 25% after FSP, which is almost 7.4 times higher than that of as-cast alloy. The impact toughness of the as-cast alloy increases from $1.2\ \text{J/cm}^2$ to about $8.3\ \text{J/cm}^2$ after FSP, which is almost 7 times higher than that of the as-cast alloy. This improvement in all properties was mainly attributed to the refinement and morphological changes in eutectic silicon particles.
3. While brittle fracture is the main failure mechanism in the as-cast alloy samples, this transforms into the ductile fracture mode for both tensile and Charpy tests after FSP. It can be concluded from the results that FSP effectively transforms the as-cast brittle Al-12Si alloy into a tougher alloy with ductile fracture mode.

References

- [1] G. Purcek, O. Saray, O. Kul, *Met. Mater. Int.* 16 (2010) 145-154.
- [2] Z. Y. Ma, S. R. Sharma, R. S. Mishra, *Metall. Mater. Trans. A* 37 (2006) 3323-3336.
- [3] A. Ma, K. Suzuki, Y. Nishida, N. Saito, I. Shigematsu, M. Takagi, H. Iwata, A. Watazu, T. Imura, *Acta Mater.* 53 (2005) 211-220.
- [4] K. G. Basavakumar, P. G. Mukunda, M. Chakraborty, *Mater Charact.* 59 (2008) 283-289.
- [5] J. M. Garcia-Infanta, A. P. Zhilyaev, C. M. Cepeda-Jimenez, O. A. Ruano, F. Carreno, *Scripta mater.* 58 (2008) 138-141.
- [6] A. Ma, M. Takagi, N. Saito, H. Iwata, Y. Nishida, K. Suzuki, I. Shigematsu, *Mater. Sci. Eng. A* 408 (2005) 147-153.
- [7] K. G. Basavakumar, P. G. Mukunda, M. Chakraborty, *Int. J. Impact Eng.* 35 (2008) 199-205.
- [8] A. Ma, K. Suzuki, N. Saito, Y. Nishida, M. Takagi, I. Shigematsu, H. Iwata, *Mater. Sci. Eng. A* 399 (2005) 181-189.
- [9] A. Ma, Y. Nishida, K. Suzuki, I. Shigematsu, N. Saito, *Scripta mater.* 52 (2005) 433-437.
- [10] G. Purcek, O. Saray, I. Karaman, T. Kucukomeroglu, *Mater. Sci. Eng. A* 490 (2008) 403-410.
- [11] A. Azushima, R. Kopp, A. Korhonen, D. Y. Yang, F. Micari, G. D. Lahoti, P. Groche, J. Yanagimoto, N. Tsuji, A. Rosochowski, A. Yanagida, *CIRP Ann-Manuf. Techn.* 57 (2008) 716-735.
- [12] R. Z. Valiev, T. G. Langdon, *Prog. Mater. Sci.* 51 (2006) 881-981.
- [13] Z.Y. Ma, *Metall. Mater. Trans. A* 39 (2008) 642-658.
- [14] R. S. Mishra, M. W. Mahoney, *Friction Stir Welding and Processing*, Chapter 1: Introduction, ASM Int. 2007 pp. 1-5.
- [15] R.S. Mishra, Z.Y. Ma, *Mater. Sci. Eng. R* 50 (2005) 1-78.
- [16] W.M. Thomas, E.D. Nicholas, J.C. Needham, M.G. Murch, P. Templesmith, C.J. Dawes: G.B. Patent Application No. 9125978.8 Dec. 1991.
- [17] Z. Y. Ma, S. R. Sharma, R. S. Mishra, *Mater. Sci. Eng. A* 433 (2006) 269-278.
- [18] S. Jana, R.S. Mishra, J.B. Baumann, G. Grant, *Acta Metall.* 58 (2010) 989-1003.

- [19] L. Karthikeyan, V.S. Senthilkumar, K. A. Padmanabhan, *Mater. Des.* 31 (2010) 761-771.
- [20] F.Y. Tsai, P.W. Kao, *Mater. Lett.* 80 (2012) 40-42.
- [21] M. M. E. Rayesa, E. A. E. Danafa, *J. Mater. Process. Technol.* 212 (2012) 1157-1168.
- [22] A. M. H. Wais, J. M. Salman, A. O. A. Roubaiy, *Int. J. Sci. Res.* 2 (2013) 2319-7064.
- [23] S. Tutunchilar, M.K. B. Givi, M. Haghpanahi, P. Asad, *Mater. Sci. Eng. A* 534 (2012) 557- 567.
- [24] T. S. Mahmoud, S. S. Mohamed, *Mater. Sci. Eng. A* 558 (2012) 502-509.
- [25] F.Y. Tsai, P.W. Kao, *Mater. Lett.* 80 (2012) 40-42.
- [26] T. S. Mahmoud, *Surf. Coat. Technol.* 228 (2013) 209-220.
- [27] A. G. Rao, B. R. K. Rao, V. P. Deshmukh, A. K. Shah, B. P. Kashyap, *Mater. Lett.* 63 (2009) 2628-2630.
- [28] S.R. Sharma, Z.Y. Ma, R.S. Mishra, *Scr. Mater.* 51 (2004) 237-241.
- [29] S. R. Sharma, R. S. Mishra, *Scr. Mater.* 59 (2008) 395-398.
- [30] S. Jana, R.S. Mishra, J.B. Baumannb, G. Grant, *Scr. Mater.* 61 (2009) 992-995.
- [31] Z. Y. Ma, A.L. Pilchak, M.C. Juhasa, J.C. Williams, *Scr. Mater.* 58 (2008) 361-366.
- [32] M.L. Santella, T. Engstrom, D. Storjohann, T.Y. Pan, *Scr. Mater.* 53 (2005) 201-206.
- [33] Z. Y. Ma, S. R. Sharma, R. S. Mishra, *Scr. Mater.* 54 (2006) 1623-1626.
- [34] D. H. Choi, Y. H. Kim, B. W. Ahn, Y. I. Kim, S. B. Jung, *Trans. Nonferr.Met. Soc. Ch.* 23 (2013) 335-340.
- [35] Z.Y. Ma, R.S. Mishra, M.W. Mahoney, *Scr. Mater.* 50 (2004) 931-935.
- [36] S.A.Alidokht, A. A.Zadeh, S. Soleymani, T. Saeid, H. Assadi, *Mater. Charact.* 63 (2012) 90-97.
- [37] C. W. Yang, Y. H. Chang, T. S. Lui, L. H. Chen, *Mater. Des.* 40 (2012) 163-170.

TABLE CAPTIONS

Table 1. Tensile properties of the as-cast and FSPed Al–12Si alloy (σ_{UTS} : Ultimate Tensile Strength, σ_Y : Yield Strength, ϵ_f : Elongation to Failure, ϵ_u : Uniform Elongation).

FIGURE CAPTIONS

Fig.1. Schematic illustrations of the processed plate and the sample geometries taken from its inside.

Fig.2. Optical micrographs showing the microstructure of as-cast Al-12Si alloy at: (a) low and (b) high magnifications.

Fig.3. (a) A general macro-view of the cross-section of FSPed sample perpendicular to the advancing direction. Selected micrographs showing the: (b) SE-TMAZ, (c)-(d) the NZ from top of the surface through the subsurface, (e) transition region between the NZ and the PE-TMAZ just under the NZ, (f) transition region on the retreating side and (g) transition region on the advancing side.

Fig.4. Histograms showing the distribution of eutectic silicon particle's length in Al-12Si alloy: (a) as-cast and (b) FSPed.

Fig.5. Histograms showing the distribution of the aspect ratio of eutectic silicon particles in Al-12Si alloy: (a) as-cast and (b) FSPed.

Fig.6. Optical micrographs and hardness profiles of: (a)-(b) longitudinal and (c)-(d) vertical cross-sections of the FSPed sample.

Fig.7. Engineering stress–strain curves of the as-cast and FSPed Al–12Si alloy.

Fig.8. SEM micrographs showing the fracture surfaces of tension samples: (a) As-cast sample and (b) FSPed sample.

Fig.9. Optical micrographs showing the crack paths and sub-surface microstructures of the tensile tested samples of Al-12Si alloy: (a) as-cast sample and (b) FSPed sample.

Fig.10. Absorbed energy of Al-12Si alloy in the as-cast and FSPed conditions.

Fig.11. Pictures showing the fracture surfaces of: (a) as-cast and (b) FSPed samples after impact testing. SEM micrographs showing detailed microstructures of fractured surfaces after impact testing of: (c) As-cast and (d) FSPed samples.

Table 1. Tensile properties of the as-cast and FSPed Al-12Si alloy (σ_{UTS} : Ultimate Tensile Strength, σ_Y : Yield Strength, ϵ_f : Elongation to Failure, ϵ_u : Uniform Elongation).

Condition	Properties				
	σ_{UTS} (MPa)	σ_Y (MPa)	ϵ_f (%)	ϵ_u (%)	σ_{UTS}/σ_Y
As-cast	167 ± 6	109 ± 5	3.4 ± 0.3	2.7 ± 0.5	1.50
FSPed	215 ± 3	131 ± 4	25.0 ± 1.1	15.0 ± 0.6	1.60

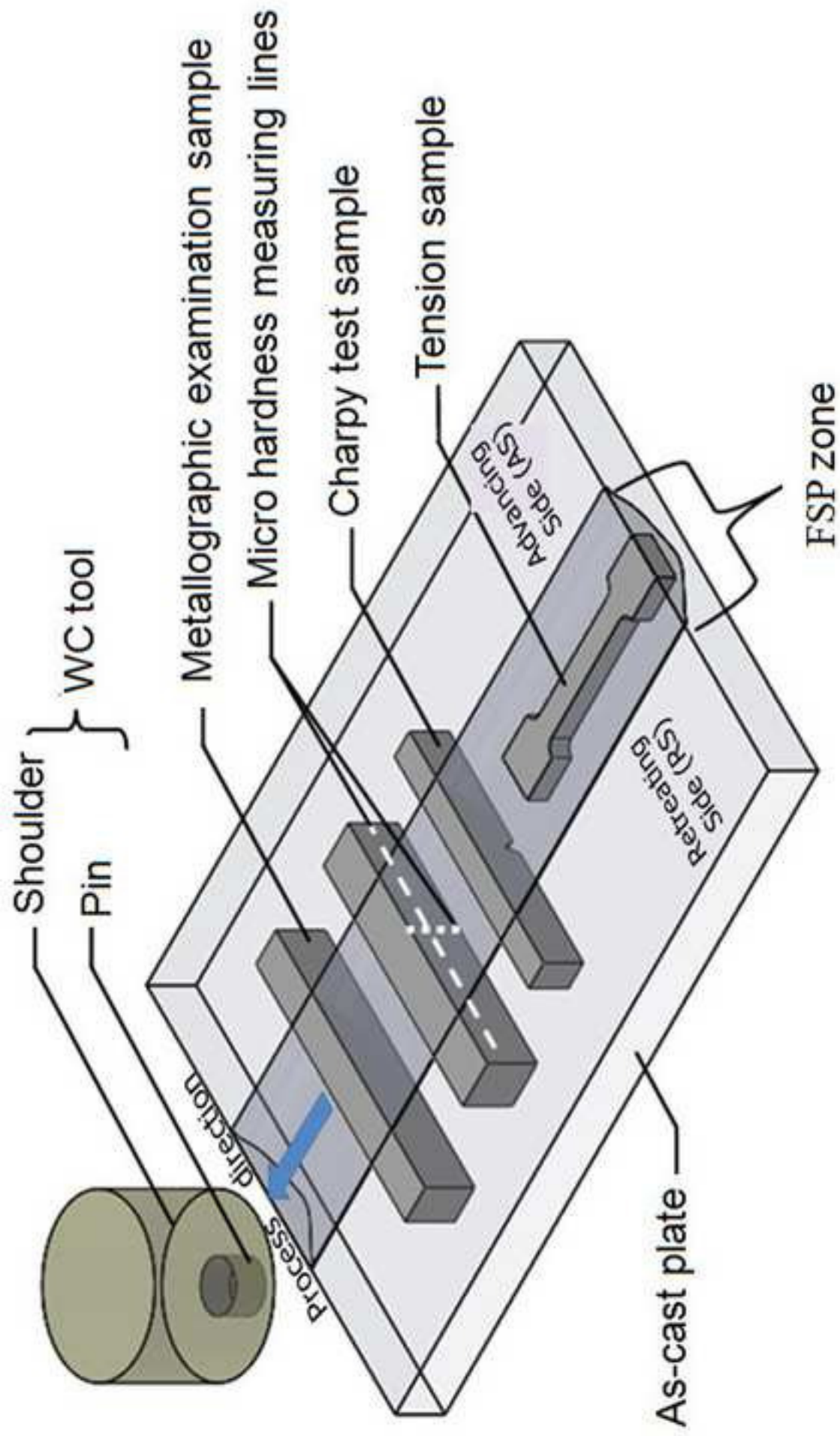


Fig.1

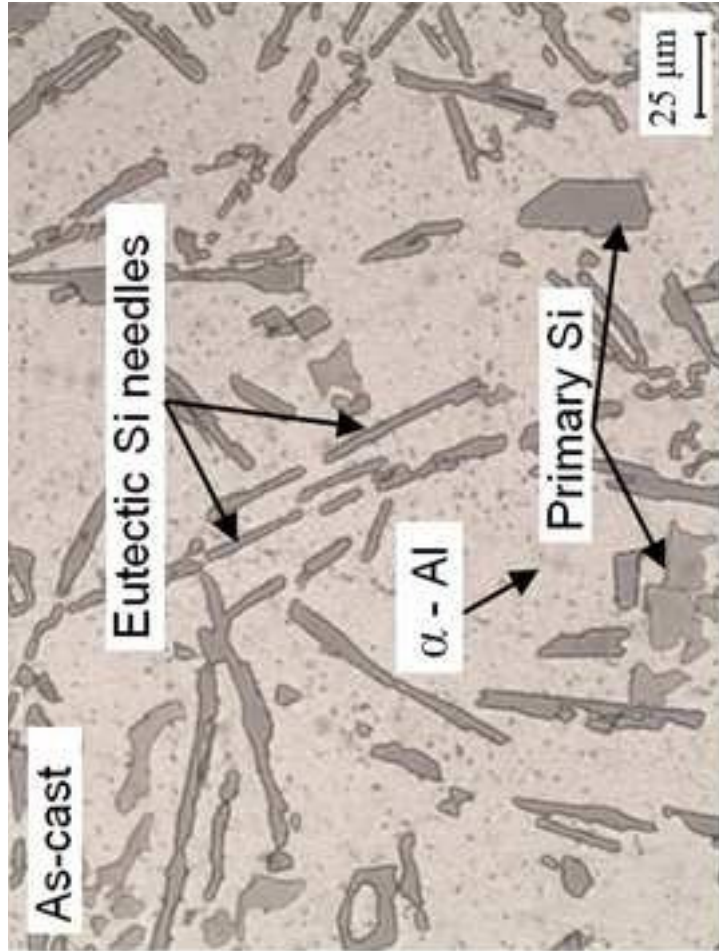


Fig.2

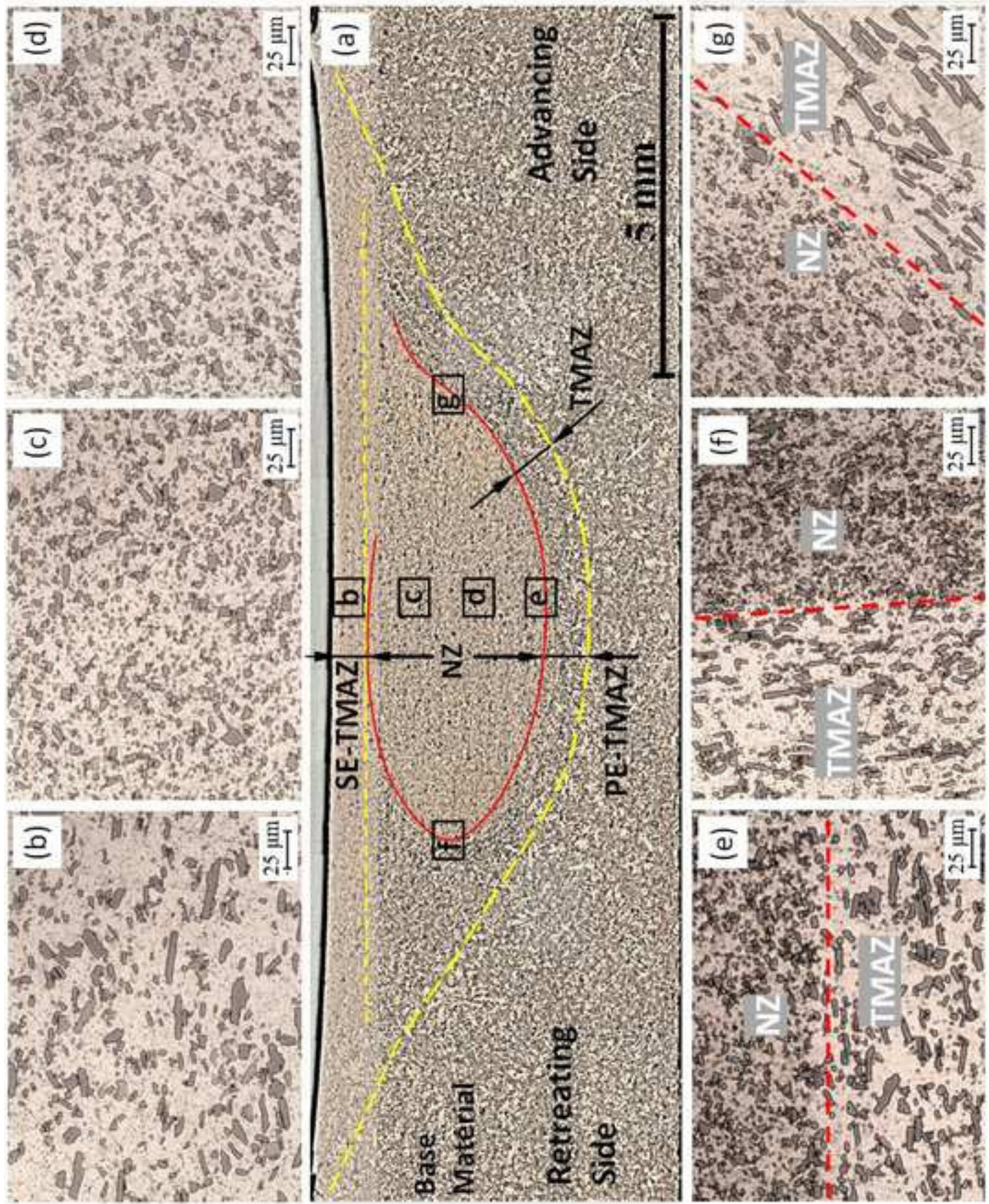


Fig.3

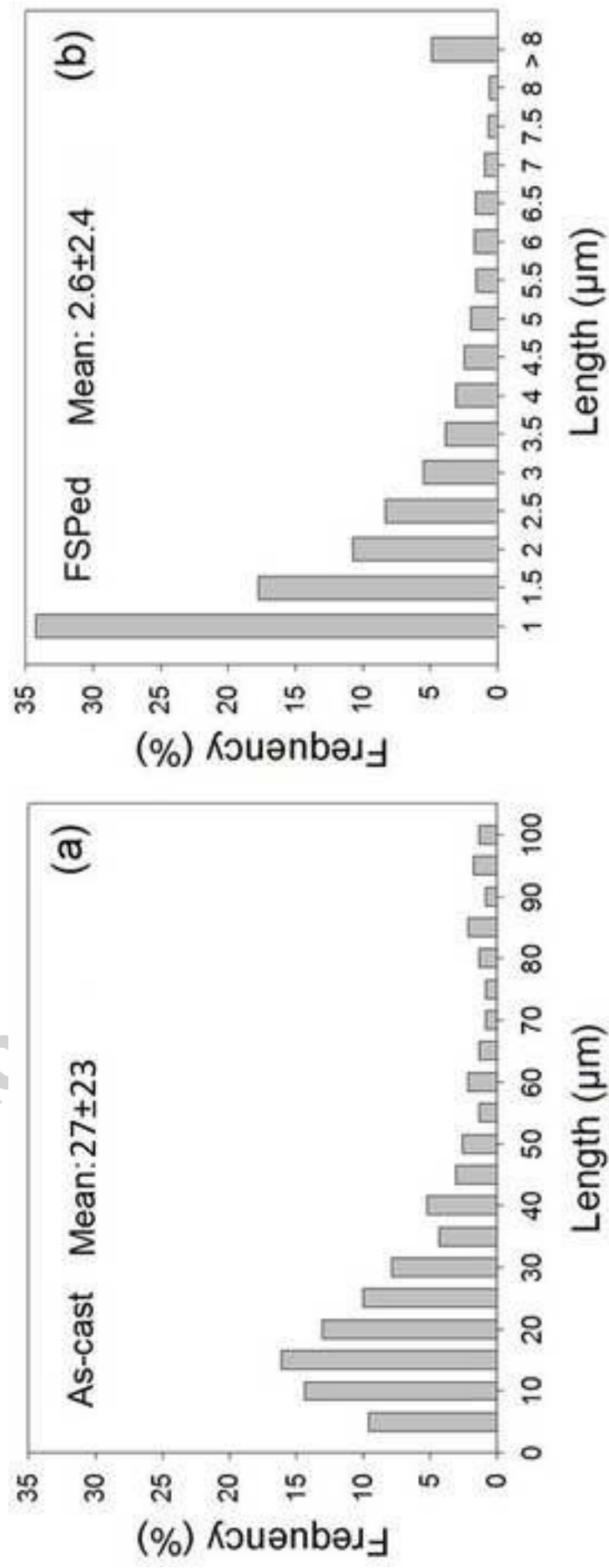


Fig.4

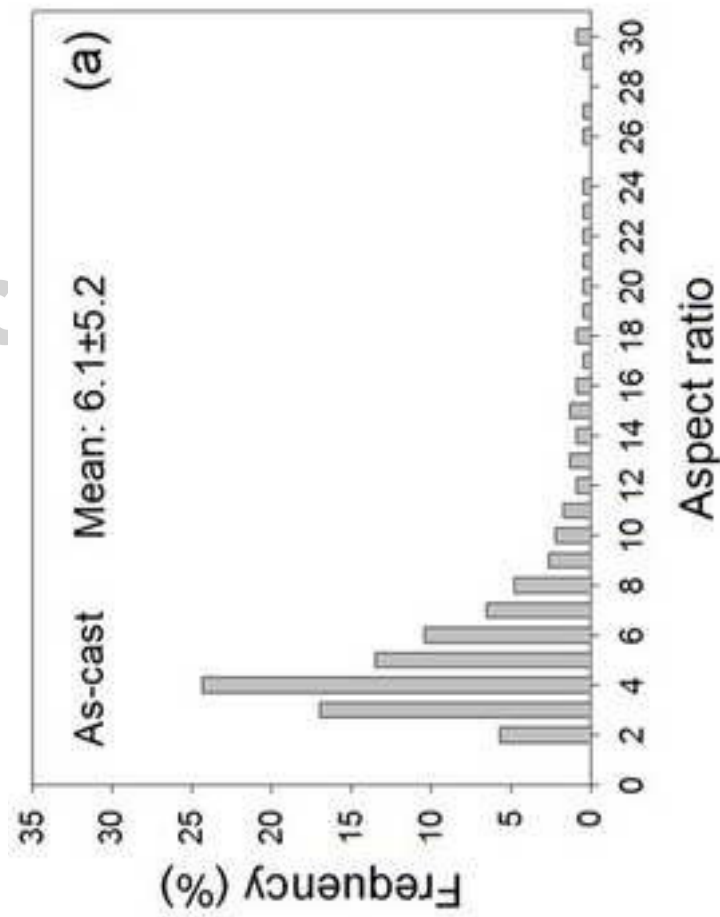
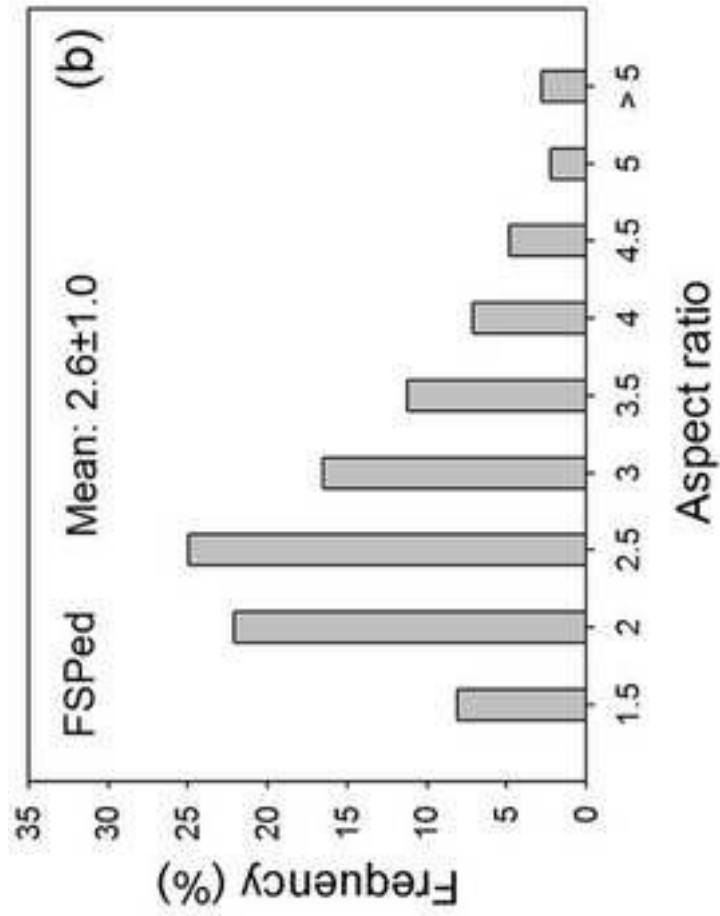


Fig.5

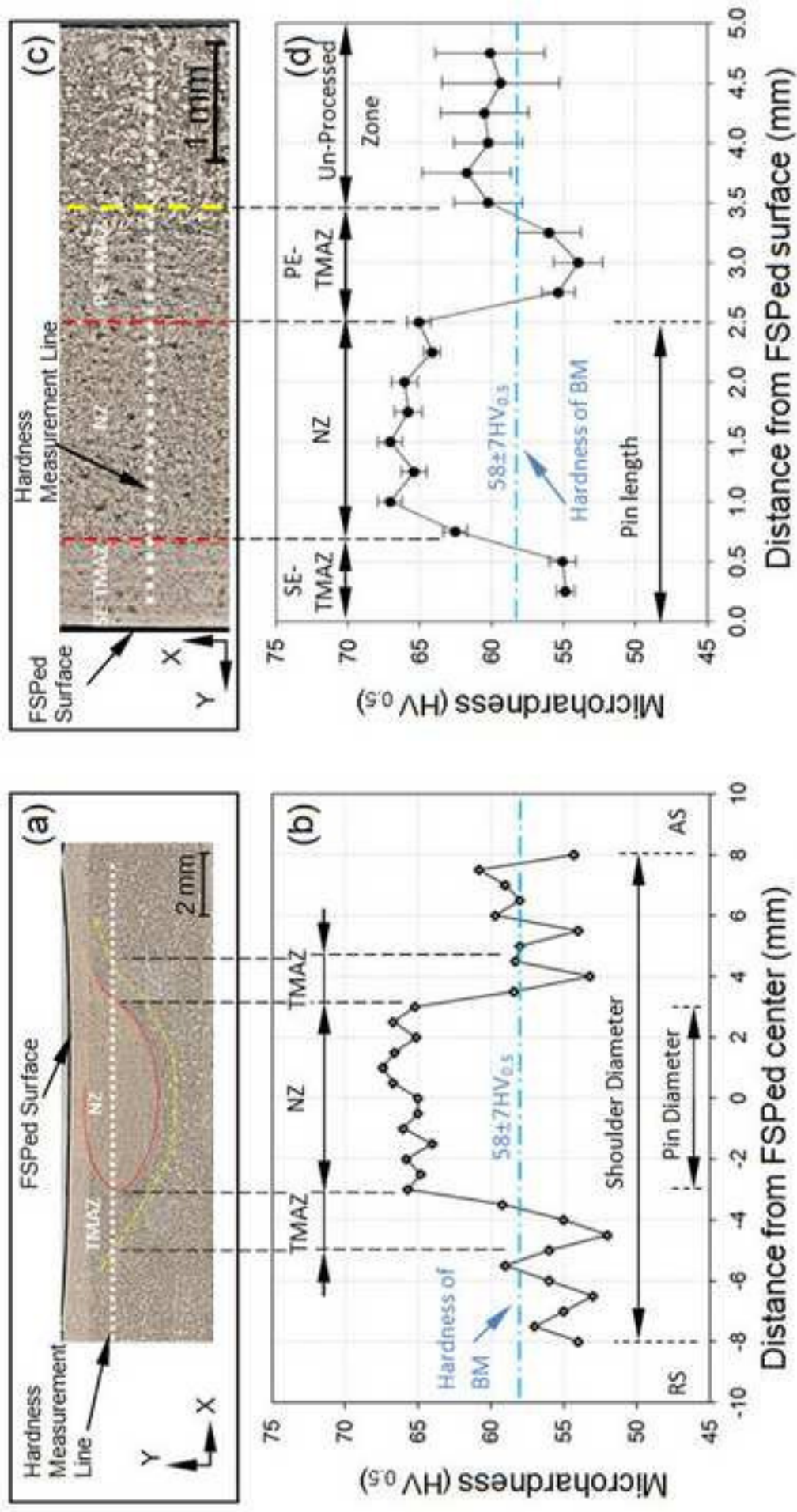


Fig.6

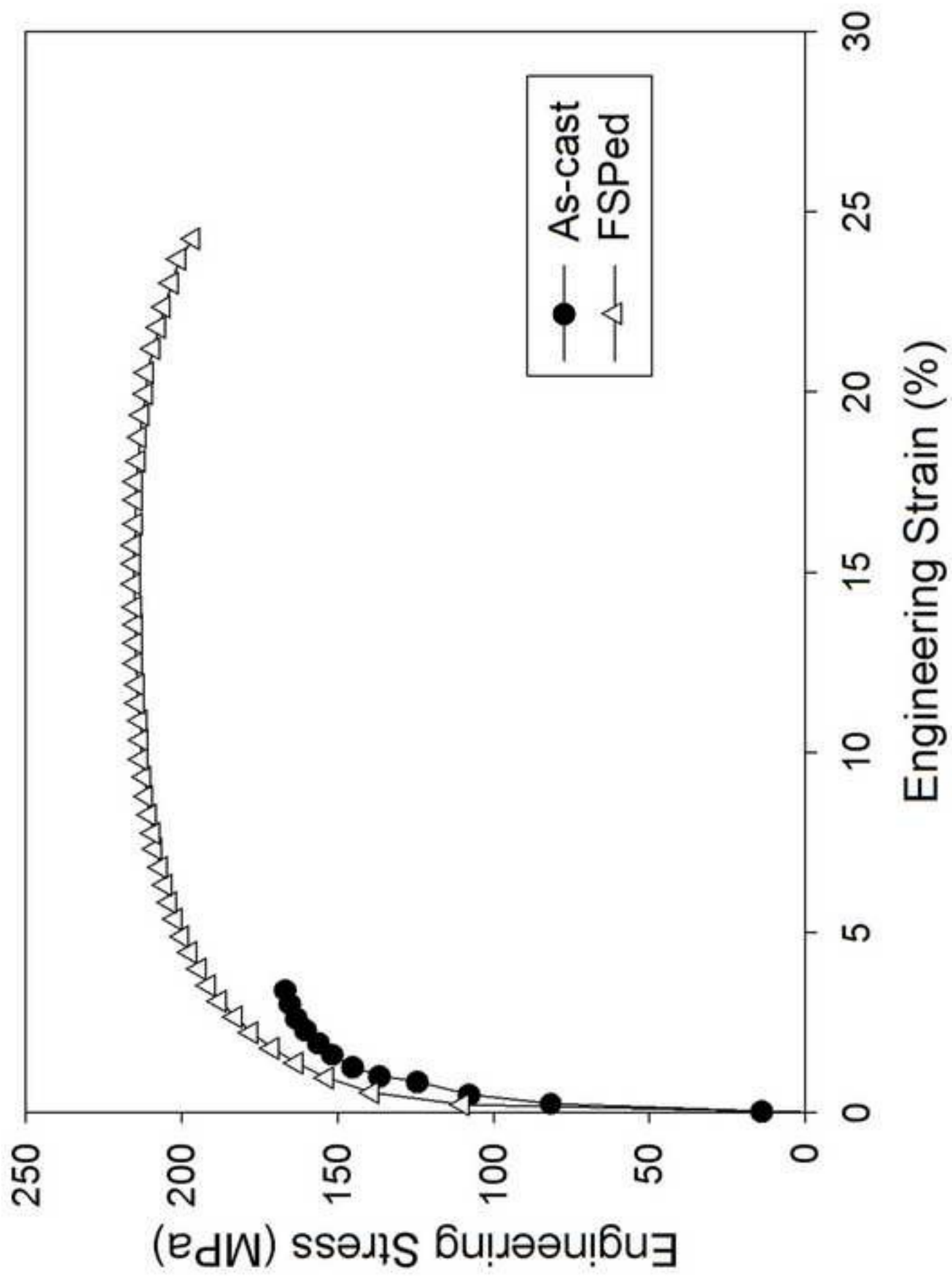


Fig.7

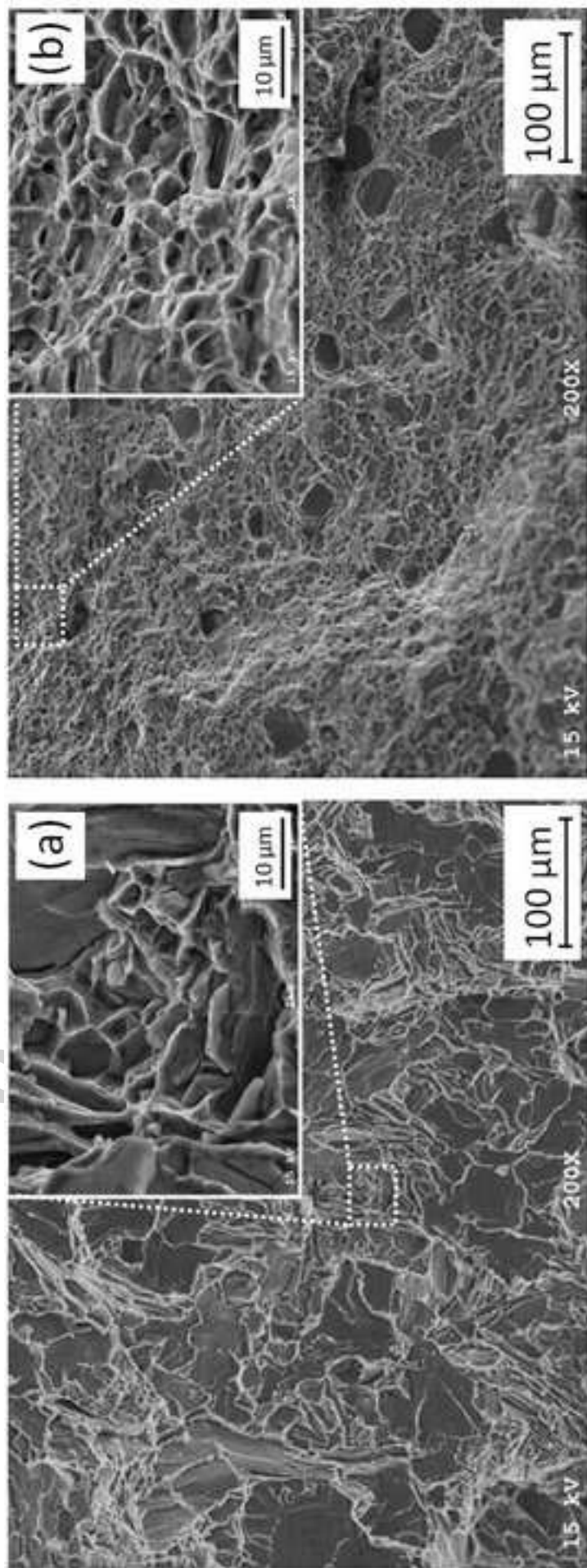


Fig.8



